

# Variational Approach for Joint Optic-Flow Computation and Video Restoration

Tal Nir      Ron Kimmel      Alfred Bruckstein  
 Department of Computer Science  
 Technion—Israel Institute of Technology  
 Technion City, Haifa 32000, Israel  
 {taln, ron, freddy}@cs.technion.ac.il

## Abstract

*We introduce a variational approach for simultaneous optical flow computation and video denoising. The proposed functional includes optical flow terms that depend on the restored sequence and an image sequence restoration term that depends on the optical flow. Our functional results in coupled Euler-Lagrange equations that are solved simultaneously for both the optical flow and the image sequence. The main novelty is the bidirectional coupling of the two problems. Traditional optical flow methods usually pre-filter the sequence, an operation which does not depend on the computed flow. At the other end, in image restoration, most methodologies compute the optical flow as a pre-processing stage which is independent of the restoration procedure. Here, we formulate the dependency of the optical flow and image restoration problems for the denoising and deconvolution problems. Our experiments demonstrate that the new method achieves better optical flow estimation under substantial noise levels compared to previously reported results.*

## 1. Introduction

Optical flow computation is probably as old as computer vision. It is useful for various applications like stereo matching, video compression, object tracking, and object segmentation. Several approaches have been proposed for its computation. Lucas and Kanade [13] tackled the aperture problem by solving for the parameters of a constant motion model over image patches. Horn and Schunck [11] were the first to use functional minimization for solving optical flow problems employing mathematical tools from calculus of variations. Their pioneering work offered the basic idea for solving dense optical flow fields for the whole image by using a functional with two terms: A data term penalizing for deviations from the optical flow equation, and a smoothness term penalizing for variations in the flow field. Several important modifications have been proposed following their work. Nagel [16, 17] proposed an oriented smoothness term

that penalizes anisotropically variations in the flow field according to the direction of the intensity gradients. Replacing quadratic penalty by robust statistics integral measures was proposed in [6, 8] in order to allow sharp discontinuities in the optical flow solution along motion boundaries. Using multi-frame formulations instead of the two-frames formulation allowed to use a spatio-temporal smoothness instead of the original spatial smoothness term [5, 10, 16, 23]. Brox-Bruhn-Papenberg-Weickert [7] demonstrated the importance of using the exact optical flow equation instead of its linearized version and added gradient constancy to the data term which is important in the presence of scene illumination changes. [24] is the first to propose changing the image sequence along with the computation of the optical flow using optimal control methodologies. Here, we propose to tackle the optical flow and image restoration problems in a unified approach within a variational framework. The basic idea comes from looking at the errors in the data term. These errors can be roughly classified into two main categories, errors in the computed flow field, and errors in the image itself caused by noise, optical blur, lossy compression, interlacing, etc. We propose a variational formulation of the problem that solves simultaneously for both the optical flow and the restored image sequence. In traditional optical flow computation, the images are pre-filtered. This pre-filtering is independent of the computed flow. While in image restoration, some methodologies first compute the optical flow (see for example [9]) as a pre-processing stage which is independent of the restored images.

The paper is organized as follows: In Section 2 we introduce our framework for combined denoising and optical flow computation. Section 3, discusses parameter settings and implementation considerations. Section 4 describes the experiments conducted to evaluate our method. Finally, Section 5 concludes the paper.

## 2. Problem Formulation

Given an image sequence  $I_0 : \Omega \in R^2 \times [0, T] \rightarrow [0, 1]$ , which is a sum of  $I^c$ , an (unknown) clean image sequence,

and  $n$  that represents noise, so that at each point in space-time  $I_0(x, y, t) = I^c(x, y, t) + n(x, y, t)$ , we wish to find the *dense optical flow field*  $\{u(x, y, t), v(x, y, t)\}$  and an image sequence  $I$ , so that  $I$  approximates  $I^c$  and  $I(x, y, t)$  is approximated in the best possible way by  $I(x + u(x, y, t), y + v(x, y, t), t + 1)$ . Here we discretized  $t$  to be the frame index and without loss of generality assume  $dt = 1$ . Again, the given noisy image sequence will be denoted by  $I_0$ , while  $I$  will be used as an argument for our optimization procedure and represent the denoised video which we would like to push as close as possible to  $I^c$ .

## 2.1. Traditional optical flow functionals

Traditional optical flow functionals usually include two terms: a data term  $E_D(u, v)$ , that measures the deviation from the optical flow equation, and a regularization smoothness term  $E_S(u, v)$  that quantifies the smoothness of the flow field. Overall, the flow field solution should minimize the sum of the data and smoothness terms.

$$E(u, v) = E_D(u, v) + E_S(u, v) \quad (1)$$

The main difference between the various variational methods is in the choice for the data and smoothness terms, and the numerical methods used for solving the minimizing flow field  $\{u(x, y, t), v(x, y, t)\}$ .

## 2.2. Joint optic-flow and video restoration

The functional given in Equation (5) is minimized with respect to the optical flow  $\{u, v\}$ . In fact, almost all optical flow integral measures in the literature are minimized with respect to the optical flow functions  $\{u, v\}$  alone. Let us note that there are two sources for errors in the data term,

1. errors in the flow field, and
2. errors in the image sequence due to noise, blur, interlacing, and lossy compression.

Writing the functional as depending only on the optical flow is appropriate mainly for ideal sequences generated by computer graphics procedures. In presence of errors in the image sequence, we should minimize with respect to the optical flow  $\{u, v\}$  as well as the image sequence. Although, in later sections we make specific choices for the data and smoothness terms, one could employ our approach on any of the optical flow functionals suggested in the literature. The general structure of the proposed functional is

$$E(u, v, I) = E_D(u, v, I) + E_S(u, v) + E_F(I, I_0). \quad (2)$$

The functional  $E(u, v, I)$  is minimized with respect to the flow field and the image sequence. Here,  $E_D(u, v, I)$

is the gray level time-constancy data term and is treated explicitly as a function of the image sequence.  $E_S(u, v)$  is the flow field smoothness term. The additional fidelity term  $E_F(I, I_0)$  penalizes for deviations from the measured sequence. It is vital for keeping the sequence close to the given input video. Ignoring this term, one can produce many image sequences for which the data and smoothness terms both vanish, yet, have little in common with the original sequence and flow field. For example, the trivial solution  $I(x, y, t) = 0, u(x, y, t) = 0, v(x, y, t) = 0$ , is a global minimum for a functional without the fidelity term.

## 2.3. Specific choice of the functional

We choose to use the functional proposed in [7] excluding only the gradient constancy element from the data term. The data term is

$$E_D(u, v) = \int \Psi((I(\mathbf{x} + \mathbf{w}) - I(\mathbf{x}))^2) d\mathbf{x} \quad (3)$$

Where,  $\mathbf{x} = (x, y, t)^T$  and  $\mathbf{w} = (u, v, 1)^T$ . The function  $\Psi(s^2) = \sqrt{s^2 + \varepsilon^2}$  induces an  $L_1$  metric on the data term as  $\varepsilon$  approaches zero.

The smoothness term is given by

$$E_S(u, v) = \alpha \int \Psi(\|\nabla_3 u\|^2 + \|\nabla_3 v\|^2) d\mathbf{x}. \quad (4)$$

Where  $\nabla_3$  denotes the spatio-temporal gradient. Coupling these two terms, the integral measure we would like to minimize is

$$E(u, v) = E_D(u, v) + E_S(u, v). \quad (5)$$

Finally, we add the fidelity term, treat the data term as a function of  $u, v, I$  and rewrite the functional as

$$E(u, v, I) = E_D(u, v, I) + E_S(u, v) + E_F(I). \quad (6)$$

The data term is the same as in Equation (3), the only difference is that now the image sequence is treated as a variable in the minimization process. The smoothness term of the flow field remains the same and depends only on the flow. The fidelity term penalizes for deviations from the initial given noisy sequence. We choose a quadratic term similar to the total variation denoising methodology [18],

$$E_F(I) = \lambda \int (I - I_0)^2 d\mathbf{x}. \quad (7)$$

The above fidelity term is appropriate for denoising. However, if in addition to noise, the images were degraded by a linear shift invariant filter with a given kernel  $h$ , then, the fidelity term can be modified to

$$E_F(I) = \lambda \int (h * I - I_0)^2 d\mathbf{x}. \quad (8)$$

In this case, the restored sequence filtered by  $h$  should be close to the initial given sequence  $I_0$  while the optical flow is calculated with respect to the restored sequence  $I$ .

We combined the two integral measures,

- the optical flow computation, and
- the sequence restoration.

The optical flow module receives as an input an image sequence  $I$  and computes its  $\{u, v\}$  flow. The sequence restoration module operates on the measured image sequence  $I_0$  and an optical flow field  $\{u, v\}$ , and computes the restored sequence  $I$ . Coupling the two modules is performed by feeding the optical flow from the first module to the second one. The resulting restored sequence is supplied as an input for the optical flow module. We iterate between these two procedures several times in order to refine the solution.

The optical flow module solves the Euler-Lagrange equations with respect to  $u$  and  $v$ , that is,

$$\Psi'(I_z^2)I_xI_z - \alpha \cdot \text{div}(\Psi'(\|\nabla_3u\|^2 + \|\nabla_3v\|^2)\nabla_3u) = 0$$

$$\Psi'(I_z^2)I_yI_z - \alpha \cdot \text{div}(\Psi'(\|\nabla_3u\|^2 + \|\nabla_3v\|^2)\nabla_3v) = 0$$

The numerical solution of the Euler-Lagrange equations is similar to the one described in [7], see next section for more details.

The denoising restoration scheme is derived in the following way. First, we approximate the integral by a discrete summation. Next, we use bilinear approximation in each term in the summation when required. Finally, each term in the summation is differentiated with respect to the sequence elements on which it depends. The result of the last step is used in a gradient descent scheme as an optimization process to iteratively refine the sequence volume elements.

Next, consider,

$$\int \lambda(I - I_0)^2 + \Psi((I(\mathbf{x} + \mathbf{w}) - I(\mathbf{x}))^2) d\mathbf{x}. \quad (9)$$

The discrete approximation of this integral is given by

$$\sum \lambda(I - I_0)^2 + \Psi((I(\mathbf{x} + \mathbf{w}) - I(\mathbf{x}))^2). \quad (10)$$

Let us use bilinear approximation for  $I(\mathbf{x} + w)$  in the summation of Equation (10). We have that,

$$\lambda(I - I_0)^2 + \Psi((A \cdot I_1 + B \cdot I_2 + C \cdot I_3 + D \cdot I_4 - I)^2) \quad (11)$$

where,

$$\begin{aligned} I &= I(x, y, t) \\ I_1 &= I(x_1, y_1, t + 1) \end{aligned}$$

$$\begin{aligned} I_2 &= I(x_1 + 1, y_1, t + 1) \\ I_3 &= I(x_1, y_1 + 1, t + 1) \\ I_4 &= I(x_1 + 1, y_1 + 1, t + 1) \\ x_1 &= \lfloor x + u \rfloor \\ y_1 &= \lfloor y + v \rfloor \end{aligned}$$

Again, note that here we assume w.l.o.g.  $dx = dy = dt = 1$ .

Differentiating Equation (11) with respect to each of the five image variables is straightforward. Each element in the summation of (10) depends on one image entry at frame  $t$  and four image entries at  $t + 1$ .

Note that each pixel value in the sequence volume may influence several optical flow paths and therefore collect several contributions from different terms in the summation of equation (10).

$A, B, C, D$  are the bilinear interpolation coefficients and depend only on the optical flow at  $x, y, t$ . Therefore,  $A, B, C, D$  do not change during the image restoration iterations, as the optical flow solution is numerically frozen during these iterations.

$$\begin{aligned} A &= 1 - dy - dx + dx \cdot dy; & B &= dx - dx \cdot dy \\ C &= dy - dx \cdot dy; & D &= dx \cdot dy \\ dx &= x + u - x_1; & dy &= y + v - y_1. \end{aligned}$$

Note that in the restoration phase, the data term yields smoothing of the image sequence along the optical flow trajectories.

### 3. Implementation details

We implemented the optical flow methodology of [7], with the following exceptions.

1. We excluded the gradient constancy from the data term.
2. In the multi-resolution we used an image reduction factor of 0.5 instead of 0.95.
3. We used one loop of iterations instead of dividing the loops into three levels of iterations. We used 600 iterations for each optical flow calculation.

As for the denoising module, if we choose  $\lambda \rightarrow \infty$ , then the sequence is forced to be identical to the original one which is equivalent to all existing optic flow calculation. If we choose  $\lambda = 0$ , then the sequence can be modified with no penalty (equivalent to no fidelity term). As explained earlier, such a selection might produce the trivial solution to  $I, v, u = 0$  as an optimal solution.

When assuming no knowledge of the noise level, we empirically found  $\lambda = 0.01$  suitable for most Gaussian noise conditions. If we have some knowledge of the noise, like an

approximation of the standard deviation, then  $\lambda$  should decrease as the noise level increases. The sequence is thereby allowed to drift further apart from the given noisy  $I_0$ . We modified the value of  $\lambda$  according to  $\lambda \sim 1/\text{NoiseSTD}$  and according to  $\lambda \sim 1/\text{NoiseSTD}^2$ . We empirically found that  $\lambda \sim 1/\text{NoiseSTD}$  gives better results, for  $\lambda = 0.4/\text{NoiseSTD}$ . In order to avoid singularities, we bounded the value of  $\lambda \leq 1$ .

A more academic approach to consider the noise level would be to enforce the constraint on the standard deviation of the restored sequence distance from the original to match the noise level standard deviation, and solve for the corresponding  $\lambda$ . Alternatives for estimating  $\lambda$  based on the noise characteristics would be explored elsewhere.

We used a gradient descent on the sequence values with a numerical step size of 0.1, and 400 iterations at each denoising phase. The iterations between the optical flow and the denoising modules is performed 12 times. For the optical flow we used central derivatives and the image derivatives were computed as recommended in [4].

## 4. Experimental Results

In this section we compare the results of the optical flow module alone to the results of the coupled optical flow and denoising modules. In all the experiments, the optical flow code and parameters are identical in both cases and the same number of optical flow iterations is performed. We also compare the optical flow for noisy data results to the best known results in the literature. In our evaluations we adopt the standard measures of Average Angular Errors (AAE) and Standard Deviation (STD). All our results are measured on all the pixels of the flow field (100% dense).

### 4.1 Yosemite sequence

In this section we applied our method to the Yosemite sequence without clouds, we used three resolution levels. Table 1 shows the noise sensitivity results for our optic flow code. Comparing to the results in table 2, we see that the optical flow estimation for noisy images improves significantly when applying the denoising part. The results reported by [7] are somewhat better than our results for the pure optic flow solution, partly due the missing gradient constancy term in our data term, and probably since the code in [7] is not yet publicly available. However, our coupled solution achieves better results with respect to the AAE measure in the presence of significant noise levels, see Figure 1 for comparison. Figure 3 shows the calculated flow field of the coupled approach under heavy noise of 40. Notice that changing  $\lambda$  according to the noise level improves the results for low noise levels compared to a constant  $\lambda$ . It is yet interesting to note that although the sequence is synthetic, when we changed  $\lambda$ , the results improved by a small

amount relative to working with the original sequence. We assume that the small amount of smoothing along the optical flow trajectories reduced the effects of the rendering algorithm used in producing the sequence. This result is also valid for other sequences we tried like the office sequence. Figure 2 shows the denoising results of the coupled solution, the noise standard deviation is reduced from 40 in the original sequence to 18 in the denoised sequence. Note that the denoising is less effective at boundary pixels at the lower left/right image since the optical flow there is fast and moves out of the image plane. Therefore, there are fewer pixels to work with in the smoothing process.

Table 1: Yosemite without clouds. Optical flow alone.

$\sigma_n$	AAE	STD
0	1.22°	1.25°
10	1.60°	1.50°
20	2.02°	1.73°
30	2.45°	2.01°
40	2.92°	2.27°

Table 2: Yosemite without clouds. Coupled solution of optical flow and sequence denoising. Left:  $\lambda = 0.4/\text{STDNoise}$ . Right: constant  $\lambda = 0.01$

$\sigma_n$	AAE	STD
0	1.20°, 1.42°	1.25°, 1.50°
10	1.29°, 1.44°	1.38°, 1.53°
20	1.55°, 1.57°	1.51°, 1.56°
30	1.86°, 1.85°	1.69°, 1.69°
40	2.17°, 2.17°	1.88°, 1.88°

Table 3: Yosemite without clouds. Results reported in [7].

$\sigma_n$	AAE	STD
0	0.98°	1.17°
10	1.26°	1.29°
20	1.63°	1.39°
30	2.03°	1.53°
40	2.40°	1.71°

### 4.2 Office sequence

Next we applied our method to the office sequence. For this, we used the coupled modules with varying  $\lambda$  and four resolution levels. Table 5 shows a significant improvement achieved by the whole scheme relative to the optic flow so-

Table 4: Yosemite without clouds. Results reported in [21].

$\sigma_n$	AAE
0	1.79°
10	2.53°
20	3.47°
40	5.34°

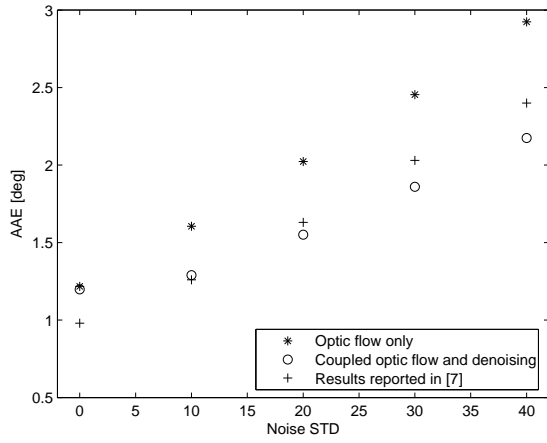


Figure 1: Yosemite sequence - noise sensitivity results.



Figure 2: Frame 8. Left-original. Middle-image with noise STD of 40. Right-denoised image.

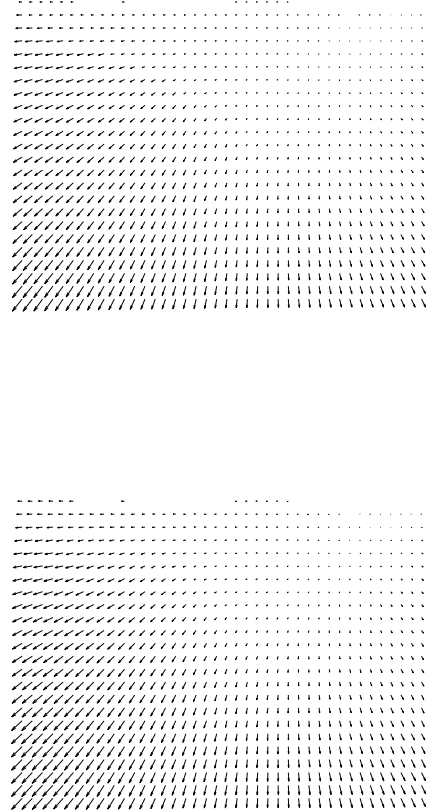


Figure 3: Optical flow of the Yosemite sequence. Upper - Ground truth. Lower - results obtained by the coupled solution with noise standard deviation of 40.

lution as a stand alone procedure. The result is 46% better in AAE for noise level 40. The improvement here is more significant than in the Yosemite sequence for two reasons: It contains more frames (higher temporal sampling rate) which provides the denoising algorithm a better support while smoothing along the optic flow trajectories. Due to the same reason, the motion field in the Yosemite sequence is larger and therefore some optic flow trajectories are shorter because they point out of the image domain. Our results for noisy sequences are significantly better than those reported in the literature (see table 6). Under heavy noise (STD= 40) our results are 78% better than the best result reported in the literature for this sequence. Figure 4 shows the denoising results obtained by our method. The noise STD in the image is reduced from 40 to 17.

Table 5: Our results on the office sequence. Left - coupled solution. Right - optic flow alone.

$\sigma_n$	AAE	STD
0	3.24°, 3.25°	3.79°, 3.79°
10	3.63°, 4.08°	3.95°, 4.14°
20	4.09°, 5.01°	4.09°, 4.52°
30	4.82°, 6.51°	4.27°, 5.13°
40	6.04°, 8.81°	4.89°, 6.48°

Table 6: Office sequence. AAE Results from the literature LK=Lucas and Kanade. HS=Horn and Schunck. CLG= Combined local global approach [21].

$\sigma_n$	LK	HS	CLG-2D	CLG-3D
0	5.75°	4.36°	4.32°	3.24°
10	6.79°	6.17°	5.89°	-
20	8.43°	8.30°	7.75°	-
40	11.47°	11.76°	10.73°	-



Figure 4: Frame 10 of the office sequence. From left to right: Original, with noise STD=40, and Denoised.

## 5. Summary and future work

In this paper we introduced the concept of simultaneously solving the optical flow and the video denoising by mini-

mizing a single functional. The results demonstrated a significant improvement of the optical flow results under noise compared to optical flow implementation without the coupled image denoising. The optical flow provides a vital information for the denoising algorithm: The knowledge about trajectories along which the image brightness should be constant. While the denoising part provides the optical flow with an improved image sequence with lower noise levels. It might be interesting in future work to test different functionals. For example, one may incorporate the gradient constancy into the data term. It would change both the optical flow as well as the denoising scheme. That is, a denoising that also tries to improve the match of the image gradients along the optical flow trajectories.

## References

- [1] L. Alvarez, J. Weickert, and J. Sanchez. "Reliable estimation of dense optical flow fields with large displacements" *International Journal of Computer Vision*, 39(1):41-56, 2000.
- [2] P. Anandan. "A computational framework and an algorithm for the measurement of visual motion" *International Journal of Computer Vision*, 2:283-310, 1989.
- [3] A. Bab-Hadiashar and D. Suter. "Robust optic flow computation" *International Journal of Computer Vision*, 29(1):59-77, 1998.
- [4] J. L. Barron, D. J. Fleet, and S. S. Beauchemin. "Performance of optical flow techniques" *International Journal of Computer Vision*, 12(1):43-77, 1994.
- [5] M. J. Black and P. Anandan. "Robust dynamic motion estimation over time" In proc. IEEE Computer Society Conference on Computer Vision and Pattern Recognition, Pages 292-302, June 1991, IEEE Computer Society Press.
- [6] M. J. Black and P. Anandan. "The robust estimation of multiple motions: parametric and piecewise smooth flow fields" *Computer Vision and Image Understanding*, 63(1):75-104, 1996.
- [7] T. Brox, A. Bruhn, N. Papenberg, and J. Weickert. "High Accuracy Optical Flow Estimation Based on a Theory for Warping" In Proc. ECCV 2004, Prague, Czech Republic - T.Pajdla, J. Matas (Eds.), Lecture Notes in Computer Science, Vol.3024, Springer, Berlin, 25-36, 2004.
- [8] R. Deriche, P. Kornprobst, and G. Aubert. "Optical flow estimation while preserving its discontinuities: a variational approach" In Proc. Second Asian Conference on Computer Vision, Vol. 2, Pages 290-295, Singapore, Dec. 1995.
- [9] M. Elad, and A. Feuer, "Super-resolution reconstruction of continuous image sequence", *IEEE Trans. On Pattern Analysis and Machine Intelligence (PAMI)*, 21(9):817-834, 1999.

- [10] G. Farneback. "Very high accuracy velocity estimation using orientation tensors, parametric motion, and simultaneous segmentation of the motion field" In Proc. 8th International Conference on Computer Vision, Vol. 1, Pages 171-177, Canada, July 2001. IEEE Computer Society Press.
- [11] B. K. P. Horn and B. Schunck. "Determining optical flow" *Artificial Intelligence*, 17:185-203, 1981.
- [12] S. H. Lai and B. C. Vemuri. "Reliable and efficient computation of optical flow" *International Journal of Computer Vision*, 29(2):87-105, 1998.
- [13] B. Lucas and T. Kanade. "An iterative image registration technique with an application to stereo vision" In Proc. 7th International Joint Conference on Artificial Intelligence, Pages 674-679 Canada, Aug. 1981.
- [14] E. Memin and P. Perez. "A multigrid approach for hierarchical motion estimation" In Proc. 6th International Conference on Computer Vision, Pages 933-938, India, Jan. 1998. Narosa Publishing House.
- [15] E. Memin and P. Perez. "Hierarchical estimation and segmentation of dense motion fields" *International Journal of Computer Vision*, 46(2):129-155, 2002.
- [16] H. H. Nagel. "Extending the 'oriented smoothness constraint' into the temporal domain and the estimation of derivatives of optical flow" In Proc. ECCV, Vol. 427, Lecture notes in Computer Science, Pages 139-148. Springer, Berlin, 1990.
- [17] H. H. Nagel and W. Enkelmann. "An investigation of smoothness constraints for the estimation of displacement vector fields from image sequences" *IEEE Trans. on Pattern Analysis and Machine Intelligence*, 8:565-593, 1986.
- [18] L.I. Rudin, S. Osher, and E. Fatemi. "Nonlinear total variation based noise removal algorithms" *Physica, D*, 60:259-268, 1992.
- [19] C. Schnor. "Segmentation of visual motion by minimizing convex non-quadratic functionals" In Proc. 12th International Conference on Pattern Recognition, Vol. A, Pages 661-663, Israel, Oct. 1994. IEEE Computer Society Press.
- [20] S. Uras, F. Girosi, A. Verri, and V. Torre. "A computational approach to motion perception" *Biological Cybernetics*, 60:79-87, 1998.
- [21] J. Weickert, A. Bruhn, and C. Schnorr. "Lucas/Kanade meets Horn/Schunck: Combining local and global optic flow methods" Technical Report 82, Dept. of Mathematics, Saarland Univ, Saarbrücken, Germany, Apr. 2003.
- [22] J. Weickert and C. Schnorr. "A theoretical framework for convex regularizers in PDE-based computation of image motion" *International Journal of Computer Vision*, 45(3):245-264, 2001.
- [23] J. Weickert and C. Schnorr. "Variational Optic flow computation with a spatio-temporal smoothness constraint" *Journal of Mathematical Imaging and Vision*, 14(3):245-255, 2001.
- [24] A. Borz, K. Ito, K. Kunisch, "Optimal control formulation for determining optical flow", *SIAM Journal on Scientific Computing*. 24(3): 818-847, 2002.